THE JOURNAL OF BIOLOGICAL CHEMISTRY VOL. 286, NO. 10, pp. 8633–8643, March 11, 2011
Printed in the U.S.A.

A Systematic Search for Endoplasmic Reticulum (ER) Membrane-associated RING Finger Proteins Identifies Nixin/ZNRF4 as a Regulator of Calnexin Stability and ER Homeostasis*[S]

Received for publication, October 25, 2010, and in revised form, December 20, 2010 Published, JBC Papers in Press, January 4, 2011, DOI 10.1074/jbc.M110.197459

Albert Neutzner[‡§1], Melanie Neutzner[§¶], Anne-Sophie Benischke[§], Seung-Wook Ryu[‡‖], Stephan Frank[¶], Richard J. Youle[‡], and Mariusz Karbowski[‡2]**

*From the [‡]Biochemistry Section, Surgical Neurological Branch, NINDS, National Institutes of Health, Bethesda, Maryland 20892, the [§]Department of Biomedicine, and the University Eye Clinic, University Hospital Basel, Hebelstrasse 20, 4031 Basel, Switzerland, the [¶]Department of Neuropathology, Institute of Pathology, University of Basel, Schönbeinstrasse 40, 4031 Basel, Switzerland, the [‖]Department of Bio and Brain Engineering, Korea Advanced Institute of Science and Technology, Daejeon 305-701, South Korea, and the **Center for Biomedical Engineering and Technology and Department of Biochemistry and Molecular Biology, University of Maryland School of Medicine, Baltimore, Maryland 21201*

To identify novel regulators of endoplasmic reticulum (ER)-linked protein degradation and ER function, we determined the entire inventory of membrane-spanning RING finger E3 ubiquitin ligases localized to the ER. We identified 24 ER membrane-anchored ubiquitin ligases and found Nixin/ZNRF4 to be central for the regulation of calnexin turnover. Ectopic expression of wild type Nixin induced a dramatic down-regulation of the ER-localized chaperone calnexin that was prevented by inactivation of the Nixin RING domain. Importantly, Nixin physically interacts with calnexin in a glycosylation-independent manner, induces calnexin ubiquitination, and p97-dependent degradation, indicating an ER-associated degradation-like mechanism of calnexin turnover.

The endoplasmic reticulum (ER)[3] is a major cellular site for production, folding, quality control, and distribution of proteins. Many regulatory mechanisms are in place to keep these processes in balance and therefore to ensure cellular fitness and survival, with ubiquitin-dependent protein degradation playing an important part (1). One major challenge the ER faces is an overload with unfolded or folding proteins. An excess of folding proteins in the ER triggers a cellular response called the unfolded protein response (UPR) (2, 3). UPR entails lowering of the protein load by the attenuation of protein translation and the up-regulation of chaperones thereby increasing the protein folding capacity of the cells. If the capacity of UPR is exceeded, the cell utilizes ER-associated degradation (ERAD), a system for the recognition of terminally misfolded proteins and their disposal (4). Misfolded proteins destined for ERAD are ubiquitinated by the RING domain containing ubiquitin ligases (5), Hrd1 (6), and Doa1 (7, 8), retrotranslocated across the ER membrane into the cytosol by the AAA-ATPase p97 (9), and then degraded by the 26 S proteasome.

Upon entry into the ER, most nascent polypeptides are recognized by glycosidases and modified on specific asparagine residues (Asn-Xaa-(Thr/Ser)) with the *N*-glycan $GlcNAc_2Man_9Gluc_3$ (10). Core glycosylation of nascent polypeptides decreases their overall hydrophobicity. Trimming of the terminal two glucose residues by glucosidase I allows for binding of the lectins/chaperones calreticulin and calnexin thereby facilitating the proper folding of the newly synthesized protein (10, 11).

Although the importance of regulated degradation of ER resident proteins is firmly established, only a small number of RING finger-containing ubiquitin ligases are known to be involved in such processes to date, namely SYVN1/hHrd1 (6, 12), AMFR/gp78 (13), TEB4/MARCH6 (14), RNF5/Rma1 (15), RNF77/TRIM13 (16), and RNF13 (17). Given the importance of protein metabolism and degradation in the ER and the vast number of ubiquitin ligases encoded in the human genome, we asked whether other ubiquitin ligases are involved in the regulation of ER-related degradation processes.

Based on the assumption that the ER lumen is devoid of E1 and E2 ubiquitination activity and on the fact that all known ubiquitin ligases on the ER possess a RING finger domain, we compiled a list of all human RING finger-containing proteins with at least one predicted transmembrane region (RTM). We found that 24 of 49 analyzed RTMs localize to the ER, and we uncovered a novel regulatory mechanism for ER protein folding via the ubiquitin-dependent regulation of the steady state levels of the chaperone calnexin by the RTM Nixin/ZNRF4.

EXPERIMENTAL PROCEDURES

Cloning—PCR fragments of the genes of interest were generated using the proofreading *Pfx* DNA polymerase (Invitrogen) from either a brain cDNA library or cDNA clones purchased from Invitrogen or OpenBiosystems as templates (for the

* This work was supported, in whole or in part, by National Institutes of Health Grant RO1 GM083131 from NIGMS (to M. K.).

[S] The on-line version of this article (available at http://www.jbc.org) contains supplemental Figs. S1–S3 and Tables S1 and S2.

[1] To whom correspondence may be addressed. E-mail: albert.neutzner@unibas.ch.

[2] To whom correspondence may be addressed. E-mail: mkarbowski@umaryland.edu.

[3] The abbreviations used are: ER, endoplasmic reticulum; AAA-ATPase, ATPase associated with various cellular activities; ERAD, ER-associated degradation; RTM, RING finger protein with transmembrane domain; UPR, unfolded protein response; Endo H, endoglycosidase H; PA, protease-associated.

source of template, primer sequences, and cloning strategy, see supplemental Tables S1 and S2). PCR fragments were purified, digested with the appropriate restriction enzymes, and cloned into YFP-N1 and YFP-C1 vectors (Clontech). All constructs were verified by sequencing. Inactive mutants were generated by amplification of the respective plasmid using *Pfu* Turbo DNA polymerase (Stratagene) and mutagenic primers changing the crucial histidine codons in the RING domain to tryptophan codons. Successful mutagenesis was verified by enzymatic digest and DNA sequencing.

Cell Culture and Transfection—HeLa cells were grown in DMEM supplemented with 10% heat-inactivated fetal bovine serum, 2 mM L-glutamine, 1 mM sodium pyruvate, MEM nonessential amino acids (Invitrogen), 100 units/ml penicillin, and 100 μg/ml streptomycin in 5% CO_2 at 37 °C. Cells were transfected with FuGENE 6 (Roche Applied Science) for confocal analysis or with Effectene (Qiagen) for protein lysates according to the manufacturer's instructions. Permanently transfected 293 FlpIn TRex cells were grown in DMEM supplemented with 10% tetracycline-validated fetal bovine serum (Clontech), 2 mM L-glutamine, 50 μg/ml blasticidin, and 100 μg/ml hygromycin and induced by addition of 1 μg/ml tetracycline.

Generation of Antibodies—The N-terminal part of Nixin (amino acids 1–250) was cloned into pET41a$^+$ and expressed in *Escherichia coli* BL21(DE3). Nixin(1–250)His_6 was purified under denaturating conditions using a metal affinity column, refolded, and injected into New Zealand White rabbits (Covance) for the generation of antibodies. Rabbit anti-Nixin serum was affinity-purified using Nixin(1–250)-Halo-His_6 fusion protein coupled to SulfoLink resin (Pierce) according to the manufacturer's suggestions. Biotinylated anti-Nixin antibody was prepared using Sulfo-link-NHS-Biotin (Pierce) according to the manufacturer's recommendations.

Western Blot—Cells were harvested, and protein lysates were prepared using RIPA buffer (Pierce) supplemented with 1 mM PMSF according to the manufacturer's recommendations. Protein lysates were analyzed by Western blot using rabbit anti-GFP polyclonal antibodies (Invitrogen), mouse anti-actin mAbs (Sigma), rabbit anti-calnexin polyclonal antibodies (Abcam), and rabbit anti-calreticulin polyclonal antibodies (StressGen). To perform quantitative Western blotting, samples were loaded in triplicate onto SDS-PAGE, and proteins were detected using primary antibodies and as secondary reagent anti-DyLight800-coupled anti-rabbit and anti-mouse antibodies (Pierce). Bands were visualized using an infrared-based laser scanner (LiCor) and quantified using Odyssey software (LiCor). Detection of actin (anti-actin mAbs, Sigma) or GAPDH (mouse anti-GAPDH, Santa Cruz Biotechnology) served as loading control.

Deglycosylation—Cell lysates were prepared using either RIPA or fractionation buffer (20 mM Hepes/KOH, pH 7.5, 10 mM KCl, 1.5 mM $MgCl_2$, 1 mM EDTA, 1 mM EGTA, 1 mM DTT, 250 mM sucrose, 0.1 mM PMSF), and protein concentration was measured. Equal amounts were denatured and treated for 1 h with Endo H or peptide:*N*-glycosidase F according to the manufacturer's suggestion (New England Biolabs).

Immunoprecipitation—Immunopurification of calnexin and Nixin was adapted from Ref. 18. Cells were harvested and lysed in lysis buffer (25 mM Hepes, pH 7.2, 10 mM $CaCl_2$, 1% digitonin, 20 mM iodoacetamide, 1 μg/ml pepstatin, 1 μg/ml leupeptin, 1 mM PMSF) for 30 min on ice. 800 μg of total protein from cleared lysates were mixed with 2 μl of anti-calnexin antibody and incubated overnight at 4 °C. The lysates were then incubated with 50 μl of protein A/G beads (Santa Cruz Biotechnology) for 2 h. Beads were washed three times with washing buffer (25 mM Hepes, pH 7.2, 10 mM $CaCl_2$, 0.2% digitonin) and cooked in 1× Laemmli sample buffer. Immunopurified proteins were analyzed using biotinylated rabbit anti-Nixin and rabbit anti-calnexin antibodies with streptavidin-HRP (Pierce) or anti-rabbit-HRP (Pierce) as secondary reagent. For denatured immunopurifications, protein lysates were incubated for 5 min with 1% SDS at 95 °C (19). After denaturation, lysates were diluted 1:4 in lysis buffer, and purification was performed as above.

Immunofluorescence and Confocal Microscopy—Briefly, 16–20 h after transfection, HeLa cells cultured in Lab-Tek chambered coverglass (number 1 German borosilicate; Nalge Nunc International) were fixed for 30 min at room temperature with 4% EM-grade paraformaldehyde (Electron Microscopy Sciences) in Hanks' balanced salt solution. The cells were then permeabilized with 0.15% Triton X-100 in Hanks' balanced salt solution for 20 min at room temperature, followed by blocking with 10% BSA in Hanks' balanced salt solution for 45 min at room temperature. Samples were incubated overnight at 4 °C with primary antibodies diluted in blocking buffer. The primary antibodies used for immunofluorescence studies were anti-calretinin mAbs (1:10; clone 34, BD Transduction Laboratories) and anti-calnexin polyclonal antibodies (1:500; Abcam 13504). Cells were washed three times for 15 min each with blocking buffer and then incubated for 1 h at room temperature with Alexa Fluor 594-conjugated goat anti-rabbit IgG antibodies (Invitrogen). Cell samples were washed with Hanks' balanced salt solution and used for confocal microscopy analysis. Images were acquired with a Zeiss LSM510 confocal microscope (Zeiss MicroImaging), using a 100×/NA1.45 α-Plan-FLUAR objective lens (Zeiss MicroImaging). Projections of 12-bit confocal z-sections (interval 0.25 μm) covering the entire depth of the cell were used.

Cellular Fractionation—Nixin-expressing cells were harvested from four 15-cm tissue culture dishes, resuspended in cellular fractionation buffer (20 mM Hepes/KOH, pH 7.5, 10 mM KCl, 1.5 mM $MgCl_2$, 1 mM EDTA, 1 mM EGTA, 250 mM sucrose, 0.1 mM PMSF), passed through a 25-gauge needle 45 times, and centrifuged for 10 min at 600 × *g* to remove unbroken cells and nuclei and to gain post-nuclear supernatant. Post-nuclear supernatant was centrifuged at 7000 × *g* for 10 min to pellet mitochondrion-enriched heavy membrane and heavy membrane supernatant. The heavy membrane supernatant was centrifuged in an SW60Ti swing-out rotor at 100,000 × *g* to separate the ER-containing light membrane fraction from soluble proteins (light membrane supernatant).

Fluorescence Protection Assay (20)—HeLa cells grown in Lab-Tek chambered coverglasses were transfected with expression constructs expressing YFP-tagged Nixin or hHRd1. To perform

fluorescence protease protection, cells were washed with KHM buffer (110 mM potassium acetate, 20 mM Hepes, pH 7.4, 2 mM $MgCl_2$) and imaged with a Zeiss LSM710 confocal microscope (Zeiss) using a 63×/NA1.4 α-Plan-FLUAR objective lens before and after permeabilization with 20 μM digitonin in KHM buffer (1 min) as well as after additional treatment with 6 mM trypsin (Sigma) in KHM buffer. Projections of 8-bit confocal z-sections (interval 1 μm) were quantified for fluorescence using the ZEN software (Zeiss).

RESULTS

The human genome encodes several hundred putative E3 ubiquitin ligases belonging to different protein families such as RING finger and HECT domain-containing proteins (21, 22). RING finger domain-containing ubiquitin ligases, encoded by more than 300 genes, form the largest of these protein families. RING fingers are highly conserved zinc-coordinating domains between 40 and 60 amino acids in length. These domains are thought to provide a platform for the binding of ubiquitin-conjugating enzymes to their substrates, thereby conferring substrate specificity to the ubiquitination machinery (23). Many RING finger ubiquitin ligases contain membrane-spanning domains consistent with a role in the regulation of membrane- and organelle-related processes.

Identification of ER-associated RING Finger Proteins—Until now, only a small subset of RTMs is described in the literature, and the detailed molecular mechanisms and functions of an even smaller number of RTMs are currently sufficiently understood. Knowing the complete inventory of ubiquitin ligases for specific subcellular membrane systems would allow novel approaches to study regulatory processes involving those membrane compartments. This is especially true for the ER, because its lumen is a major site for protein production and quality control and as such must depend on membrane-bound ubiquitin ligases to connect the cytosolic ubiquitination machinery with the luminal substrates. We therefore compiled a nonredundant list of the human RTMs localized to the ER. To this end, we performed an extensive data base search, using the RING domain of the peroxisome-associated RING finger E3 ubiquitin ligase peroxin 10 (PEX10; residues 273–311) (24) as input for the BLAST program (25) combined with transmembrane motif prediction using the TMHMM program (26). Using this approach, we identified 49 human loci coding for RING domain-containing proteins with at least one predicted transmembrane domain. We then searched the IPI protein database (27) and the NCBI RefSeq data base (ftp.ncbi.nih.gov) (28) with a PERL script implementing four RING domain patterns. After the elimination of duplicates, the IPI data base search resulted in 47 human loci coding for RTMs, whereas the NCBI RefSeq data base search produced 53 human loci with the desired features. The combined list of all human RTMs after these two independent data base searches includes 55 loci (supplemental Fig. S2 and Table S1).

To identify ER-localized RTMs, we transfected HeLa cells with constructs for the expression of RTMs fused to the yellow fluorescent protein (YFP) in both N- and C-terminal orientations (YFP-RTM and RTM-YFP; supplemental Table S2) followed by immunofluorescence microscopy for the endogenous

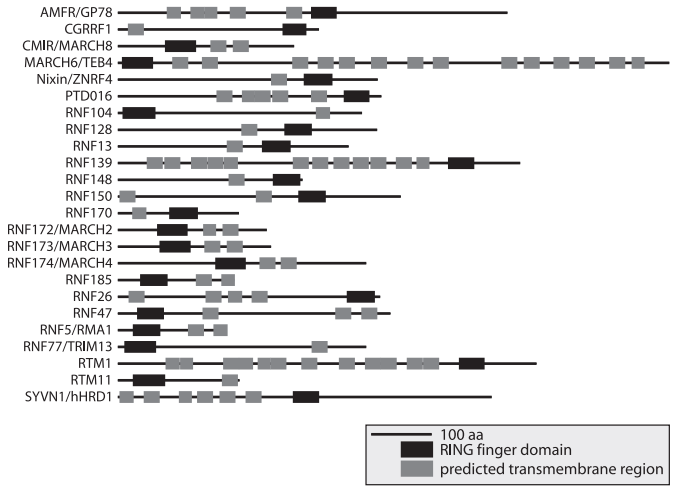

FIGURE 1. **Human ER membrane-anchored RING finger-containing proteins (RTMs).** Human cDNAs encoding putative RING finger ubiquitin ligases with at least one predicted transmembrane domain (see text) were expressed as YFP fusions in HeLa cells. The subcellular localization of the YFP fusion proteins was assessed by confocal microscopy and confirmed by immunostaining with ER-specific markers (see supplemental Fig. S1). The domain organization of the RTMs is shown drawn to scale depicting the RING domain (*black*) and predicted membrane-spanning regions (*grey*).

ER markers calnexin and calretinin. Of 48 analyzed RTMs, 24 proteins showed clear colocalization with calnexin or calretinin, suggesting an ER localization of these proteins (Fig. 1 and supplemental Fig. S1). Several other RTM constructs also yielded ER localization, but due to differences between the localization of N- and C-terminal YFP RTM fusions, we excluded these proteins from the list of ER-localized RTMs.

Nixin/ZNRF4 Is a Novel ER-localized RING Finger Ubiquitin Ligase—Nixin/ZNRF4 is a 429-amino acid protein with one predicted transmembrane region separating an N-terminal protease-associated (PA) domain and three potential *N*-glycosylation sites (NXS) from a C-terminal RING finger domain (RING) (Fig. 2*A*). Nixin was previously described as being involved in murine spermatogenesis (29) and is connected to the autosomal recessive nonsyndromic deafness locus DFNB72 (30). The ER localization of Nixin was confirmed by staining Nixin-YFP-transfected cells for calretinin as marker for the ER (Fig. 2*B*). Furthermore, subcellular fractionation revealed the presence of Nixin in the ER-enriched light membrane fraction together with the ER-localized protein calreticulin (Fig. 2*C*). To address the topology of Nixin inside the ER membrane, we performed fluorescence protease protection assays by confocal microscopy (20) of Nixin (Fig. 2*E*) and compared it with hHrd1 (data not shown) (12). The plasma membrane of HeLa cells transfected with constructs for C-terminally YFP-tagged Nixin together with ER-targeted dsRed2 was permeabilized using digitonin while leaving the ER membrane intact. Following permeabilization, cells were treated with trypsin to probe the localization of the YFP tag. We found that incubation with trypsin decreased Nixin-YFP fluorescence, although the ER lumen-localized ER-DsRed2 was protected from digestion. These data (Fig. 2*E*) and the transmembrane domain prediction based on hydrophobicity (Fig. 2*D*) argue strongly for an orientation of Nixin in the ER membrane with the N terminus containing the PA domain and three predicted glycosylation sites facing the ER

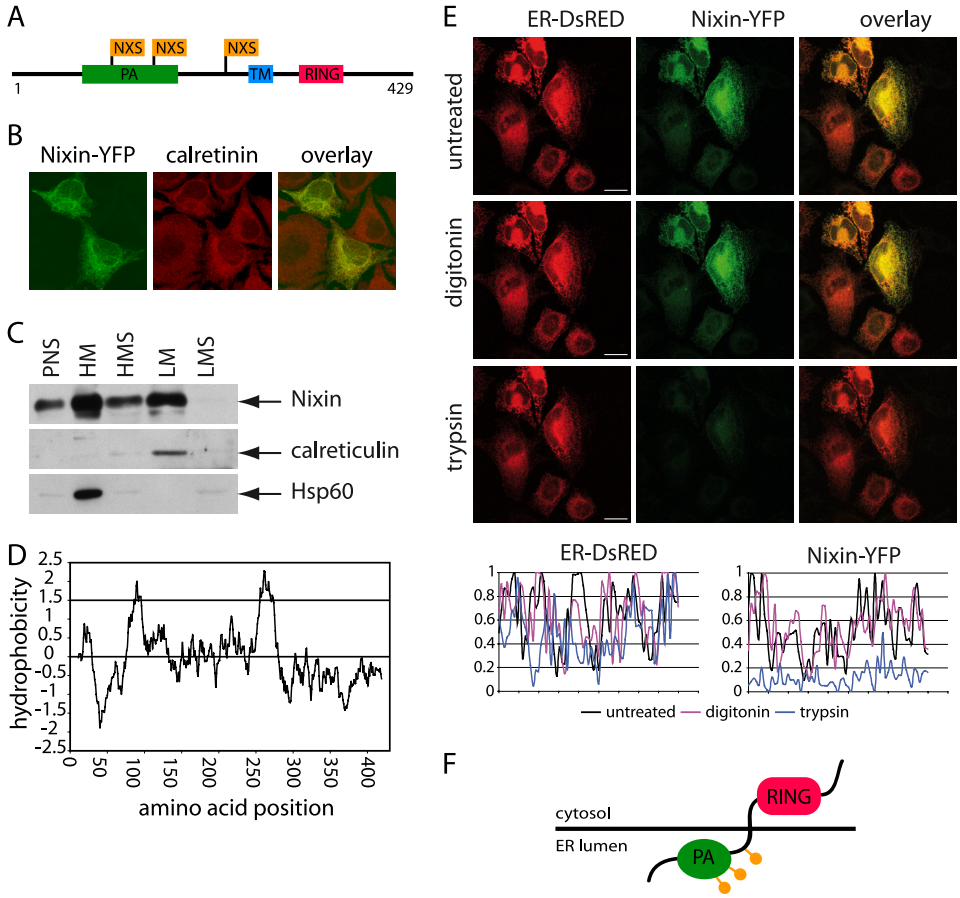

FIGURE 2. **Nixin localizes to the ER membranes.** *A,* domain organization of Nixin. Nixin contains a protease-associated domain (*green box*), one predicted transmembrane region (*TM, blue box*), a RING finger domain (*red box*), and three predicted glycosylation sides (*NXS*). *B,* Nixin localizes to the ER. HeLa cells transfected with Nixin-YFP (*green*) were fixed and stained with anti-calretinin antibodies (*red*). The *overlay* shows colocalization of Nixin with calretinin (*yellow*). *C,* protein lysates of 293 cells stably expressing wild type Nixin were fractionated by differential centrifugation into post-nuclear supernatant (*PNS*), mitochondrion-enriched heavy membrane fraction (*HM*), the ER-containing light membrane fraction, and the high speed light membrane (*LM*) supernatant (*LMS*). Nixin localization and fractionation were assessed by Western blotting using anti-Nixin antibodies. Hsp60 antibody and calreticulin antibodies were used as mitochondrial and ER markers, respectively. *D,* hydrophobic stretch in the amino acid sequence of Nixin consistent with a membrane-spanning domain was revealed by a Kyte-Doolittle hydrophobicity blot. *E,* topology of Nixin inside the ER membrane. The sensitivity of C-terminally YFP-tagged Nixin and ER lumen localized ER-DsRed toward trypsin digestion in digitonin-permeabilized cells was analyzed using confocal microscopy. Trypsin digestion-induced loss of YFP fluorescence but not of DsRed (localized in ER lumen) fluorescence argues for a cytosolic localization of the Nixin C terminus. *F,* schematic representation of the proposed ER membrane topology of Nixin.

lumen, although the C terminus with the RING domain points toward the cytosol (Fig. 2*F*; for further evidence see Fig. 3*A*).

Nixin Is a Glycoprotein—Sequence analysis of Nixin reveals the presence of three potential *N*-glycosylation sites (Asn-Xaa-(Thr/Ser)) at Asn-107 (site 1), Asn-152 (site 2), and Asn-229 (site 3) (Fig. 2*A*). Based on the observed Nixin topology inside the ER membrane (Fig. 2, *D–F*), all three sites face the ER lumen and are thus accessible by the ER-resident glycosylation machinery. Upon treatment with the glycosylation inhibitor tunicamycin (Fig. 3*A*), the mobility of Nixin on SDS-PAGE increases suggesting that Nixin is in fact glycosylated. Furthermore, treatment of lysates from FlpIn T-Rex 293 cells expressing an untagged Nixin mutant predicted to inhibit Nixin RING domain activity (H329W,H332W; Nixin^{RING-} FlpIn T-Rex 293) with the glycosidases Endo H and peptide:*N*-glycosidase F confirmed that Nixin is a target for glycosylation *in vivo* (Fig. 3*A*). Significantly, because Endo H is only active toward glycosylation stemming from the ER, but not toward glycosylation by Golgi resident enzymes (31), the susceptibility of Nixin glycosylation toward Endo H treatment confirms that Nixin is an ER-localized protein with its glycosylation sites localized in the ER lumen.

To explore a functional role of Nixin glycosylation, we generated glycosylation site mutants of Nixin by exchanging the asparagine residues in the glycosylation consensus sequences to serine. As shown in Fig. 3*B*, mutation of any one of the three asparagines led to a change in mobility of Nixin in SDS-PAGE, consistent with the conclusion that all three sites are glycosylated. In addition, mutation of Asn-107 (NixinΔG1) resulted in the generation of one major band, whereas mutation of Asn-152 (NixinΔG2) or Asn-229 (NixinΔG3) resulted in the generation of two major bands. Furthermore, although deletion of site 1 in combination with sites 2 or 3 resulted in the generation of one major band, which is presumably monoglycosylated, combining deletion of sites 2 and 3 resulted in mono- and unglycosylated Nixin. Because Nixin^{N107S,N152S,N229S} (NixinΔG1/2/3-Nixin^{Glyc-}) runs as one band, the size of Nixin from tunicamycin-treated cells, and displays the same mobility as glycosidase-treated Nixin, deletion of all three glycosylation sites appears to completely abolish Nixin glycosylation (Fig.

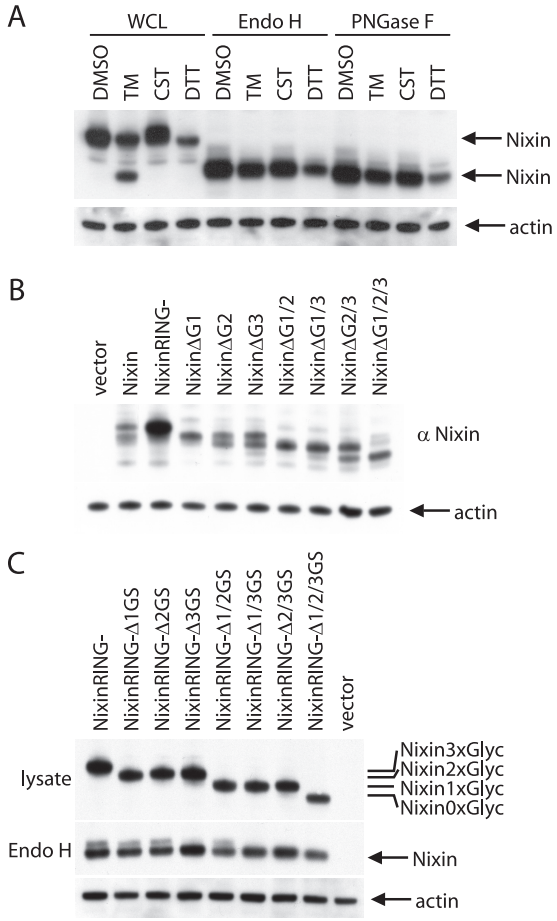

FIGURE 3. **Nixin is a glycoprotein.** *A,* to induce ER stress, 293 cells permanently expressing Nixin^{RING-} under the control of a tetracycline-inducible CMV promoter were incubated overnight with 1 μg/ml tetracycline and then treated for 3 h with tunicamycin (*TM*) or castanospermine (*CST*) or for 20 min with dithiothreitol (*DTT*). Whole cell lysates (*WCL*) obtained from these cells as well as lysates treated with the glycosidases Endo H or peptide:*N*-glycosidase F (*PNGase F*) were analyzed by Western blot using anti-Nixin or anti-actin antibodies. *B,* HeLa cells were transfected with expression constructs for wild type Nixin, Nixin^{RING-}, and all possible permutations of Nixin glycosylation site mutation (see text). At 18 h post-transfection, cells were harvested, processed for Western blot, and analyzed using anti-Nixin and anti-actin antibodies. *C,* HeLa cells transfected with expression constructs for Nixin^{RING-} or permutations of glycosylation site mutants combined with the inactivating RING mutation (see text) were lysed at 18 h post-transfection, and lysates were treated with the glycosidase Endo H or left untreated. Nixin mobility was analyzed by Western blot using anti-Nixin antibody. Actin served as loading control.

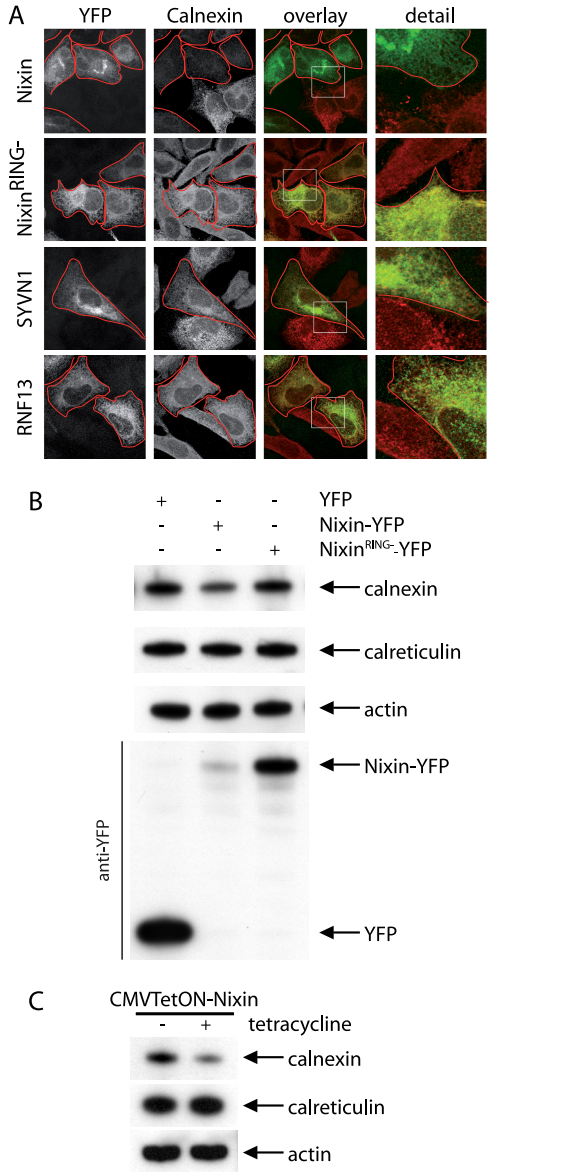

FIGURE 4. **Ectopic expression of Nixin induces down-regulation of calnexin.** *A,* HeLa cells were transfected with expression constructs for YFP-tagged: wild type Nixin, Nixin^{RING-}, SYVN1, and RNF13 (*green*), then stained with anti-calnexin antibody (*red*), and visualized by confocal microscopy. *White boxes* indicate the detail regions shown in the *right panels*. *B,* HeLa cells were transfected with expression constructs for Nixin-YFP, Nixin^{RING-}-YFP, or YFP as control, lysed, and analyzed by Western blot with anti-calnexin, anti-calreticulin, and anti-actin antibodies. *C,* FlpIn TRex 293 cells permanently transfected with Nixin under the control of a tetracycline-inducible CMV promoter were treated overnight with tetracycline or left untreated and analyzed by Western blot as described above.

3*B*). The observed heterogeneity of Nixin glycosylation suggests a preferential usage of certain sites for modification or might be related to a differential stability of the various Nixin species. To further evaluate this possibility, and because the presence of a RING domain suggests a ubiquitin ligase activity for Nixin, we inactivated the RING domain in the Nixin glycosylation mutants. We found that, unlike the mutation of glycosylation sites in wild type Nixin, combinations of glycosylation mutations (N107S and/or N152S and/or N229S) and the RING mutation (H329W,H332W) yielded homogeneous modification of the remaining glycosylation sites present in these inactive Nixin variants (Fig. 3*C*). Stabilization of Nixin by RING domain inactivation seems to allow the glycosylation of all available sites, because no additional faster migrating bands were detectable. These data would be consistent with a rather slow glycosylation of some sites (especially Asn-107-labeled N1) together with a fast turnover of Nixin with degradation of Nixin outpacing glycosylation.

Ectopic Expression of Nixin Induces RING Domain-dependent Down-regulation of Calnexin—While studying the localization of Nixin by costaining with calnexin, we found that ectopic expression of this protein dramatically reduced calnexin staining compared with other known or suspected ER-localizing RTMs (Fig. 4*A* and supplemental Fig. S1). Therefore, we hypothesized that Nixin might act as a ubiquitin ligase that facilitates proteasomal degradation of calnexin. To address this

possibility, we analyzed the effect of a Nixin variant with mutations inside the RING domain predicted to inactivate Nixin ubiquitin ligase activity (H329W,H332W; Nixin^{RING-}). As shown in Fig. 4*A*, Nixin^{RING-}-YFP colocalized with calnexin in a typical ER localization pattern, but no reduction of endogenous calnexin staining was apparent as compared with Nixin-YFP-expressing cells. This demonstrates the RING finger domain dependence of the Nixin-induced down-regulation of calnexin and again confirms the ER localization of Nixin. To evaluate the specificity of Nixin-dependent calnexin down-regulation, we analyzed calnexin immunostaining after ectopic expression of SYVN1/hHrd1, a prototypical ERAD ubiquitin ligase, and of RNF13, the closest Nixin human homolog. Neither ectopic expression of SYVN1/hHrd1 nor RNF13 had any detectable effect on the expression of calnexin as assessed by immunofluorescence (Fig. 4*A*). In contrast, expression of Nixin greatly reduced calnexin levels in over 80% of the transfected cells (Fig. 4*A*). Furthermore, of all 24 RTMs localized to the ER, only ectopic expression of Nixin led to noticeable changes in calnexin levels (supplemental Fig. S1). To independently confirm the Nixin-induced calnexin down-regulation, HeLa cells transfected with Nixin-YFP, Nixin^{RING-}-YFP, or YFP as control were analyzed by Western blot (Fig. 4*B*). Consistent with the immunofluorescence results, the Western blot analysis revealed that the expression of wild type Nixin reduced levels of calnexin in a RING finger-dependent manner. Significantly, levels of the calnexin-related lectin, calreticulin, were unaffected by ectopic expression of Nixin (Fig. 4*B*), further corroborating the specificity of Nixin-dependent degradation of calnexin. To extend the evaluation of Nixin-induced down-regulation of calnexin to other cell lines, we used a permanently transfected FlpIn T-Rex 293 cell line with untagged Nixin under the control of a tetracycline-inducible CMV promoter (Nixin FlpIn T-Rex 293). Tetracycline-mediated induction of Nixin led to the selective degradation of calnexin (Fig. 4*C*), confirming the data obtained using Nixin-YFP-expressing HeLa cells (Fig. 4*B*). Taken together, ectopic expression of Nixin induced a specific RING finger-dependent down-regulation of calnexin, indicating a role for Nixin in the regulation of calnexin levels.

Nixin-induced Calnexin Down-regulation Is Glycosylation-independent—Calnexin is a lectin, which binds glycoproteins in the ER. Therefore, we hypothesized that Nixin glycosylation (see Fig. 3) might play a role for the activity of this protein toward calnexin. To test this possibility, we examined calnexin levels after tetracycline-induced ectopic expression of Nixin^{Glyc-} in comparison with wild type Nixin and Nixin^{RING-} in permanently transfected FlpIn T-Rex 293 cells (Fig. 5*A*). We found that although ectopic expression of inactive Nixin^{RING-} caused the accumulation of calnexin to about 140% of the amount before induction, both wild type Nixin and Nixin^{Glyc-} caused the degradation of calnexin to about the same levels (around 35%) as quantified by infrared fluorescence Western blot using β-actin expression as loading control.

These data were further confirmed by immunofluorescence analysis. HeLa cells were transfected with Nixin, Nixin^{Glyc-}, and Nixin^{RING-} expression constructs, and calnexin levels were analyzed by confocal microscopy. We found that ectopic expression of wild type Nixin decreased calnexin levels (Fig. 5*B*) in 92.9 $\pm$ 2.18% of transfected cells, although expression of Nixin^{RING-} caused a noticeable decrease in calnexin levels only in 0.2 $\pm$ 0.4% of transfected cells. Like wild type Nixin, ectopic expression of Nixin^{Glyc-} caused massive calnexin degradation in 28.4 $\pm$ 4.9% of transfected cells, although it had a somewhat smaller effect on calnexin levels in 21.9 $\pm$ 2.25% of these cells, and no detectable degradation of calnexin in 49.6 $\pm$ 4.1% of the transfected cells was evident. In addition, we examined calnexin levels in cells transfected with the various Nixin expression constructs by quantitative analysis of confocal images. The data confirmed that Nixin is a potent inducer of calnexin degradation (Fig. 5*B*). Furthermore, Nixin^{RING-} is not only unable to induce calnexin degradation but also appears to act as a dominant-negative mutant interfering with calnexin turnover and therefore stabilizes calnexin in a subset of cells (Fig. 5*B*; 82% of Nixin^{RING-} cells have a higher than average calnexin staining when compared with vector control cells). As for Nixin^{Glyc-}, we noticed that the levels of expression of this protein are somewhat lower compared with the wild type protein. This may account for the robust strong down-regulation of calnexin in the permanent Nixin^{Glyc-} FlpIn T-Rex 293 cells compared with the variable down-regulation in transiently transfected HeLa cells. Taken together, although a functional RING domain is essential for calnexin degradation, glycosylation of Nixin is dispensable for its activity, arguing for lectin/carbohydrate interaction-independent calnexin recognition by Nixin.

Mechanism of Nixin-mediated Calnexin Degradation—To gain further insight into the Nixin-induced degradation of calnexin, we tested whether Nixin shares properties with other RING finger ubiquitin ligases. One hallmark of ubiquitin ligases is their ability to mediate their own degradation. Inactivation of the RING domain is therefore predicted to prevent autodegradation and promote stability of RING finger ubiquitin ligases (32). HeLa cells were transfected with expression constructs for Nixin or Nixin^{RING-} and treated with either the proteasome inhibitor MG132 or mock-treated with DMSO. As shown in Fig. 6*A*, MG132 stabilizes Nixin, arguing for a role of the proteasome in the regulation of wild type Nixin levels. Additionally, consistent with a role of Nixin in its own degradation, inactivation of the RING finger domain increased stability of Nixin, strongly arguing for a ubiquitin ligase activity of this protein (Fig. 6*A*). To analyze whether the observed down-regulation of calnexin after Nixin expression is due to proteasomal degradation of calnexin, we expressed Nixin in the presence and absence of the proteasome inhibitor MG132 and analyzed calnexin levels using a quantitative infrared fluorescence-based Western blot (Fig. 6*B*). Although expression of Nixin caused calnexin levels to drop to around 40% of the steady state value, treatment with the proteasomal inhibitor MG132 prevented calnexin degradation. Thus, Nixin induces a proteasome-mediated degradation of calnexin.

In addition, degradation and ubiquitination of calnexin were analyzed by Western blot during a time course of Nixin expression in Nixin FlpIn T-Rex 293 cells (Fig. 6*C*). These experiments revealed that elevated levels of Nixin were apparent as early as 1 h after tetracycline addition, with full induction of Nixin at 5–6 h after tetracycline addition. Notably, after 4 h of Nixin

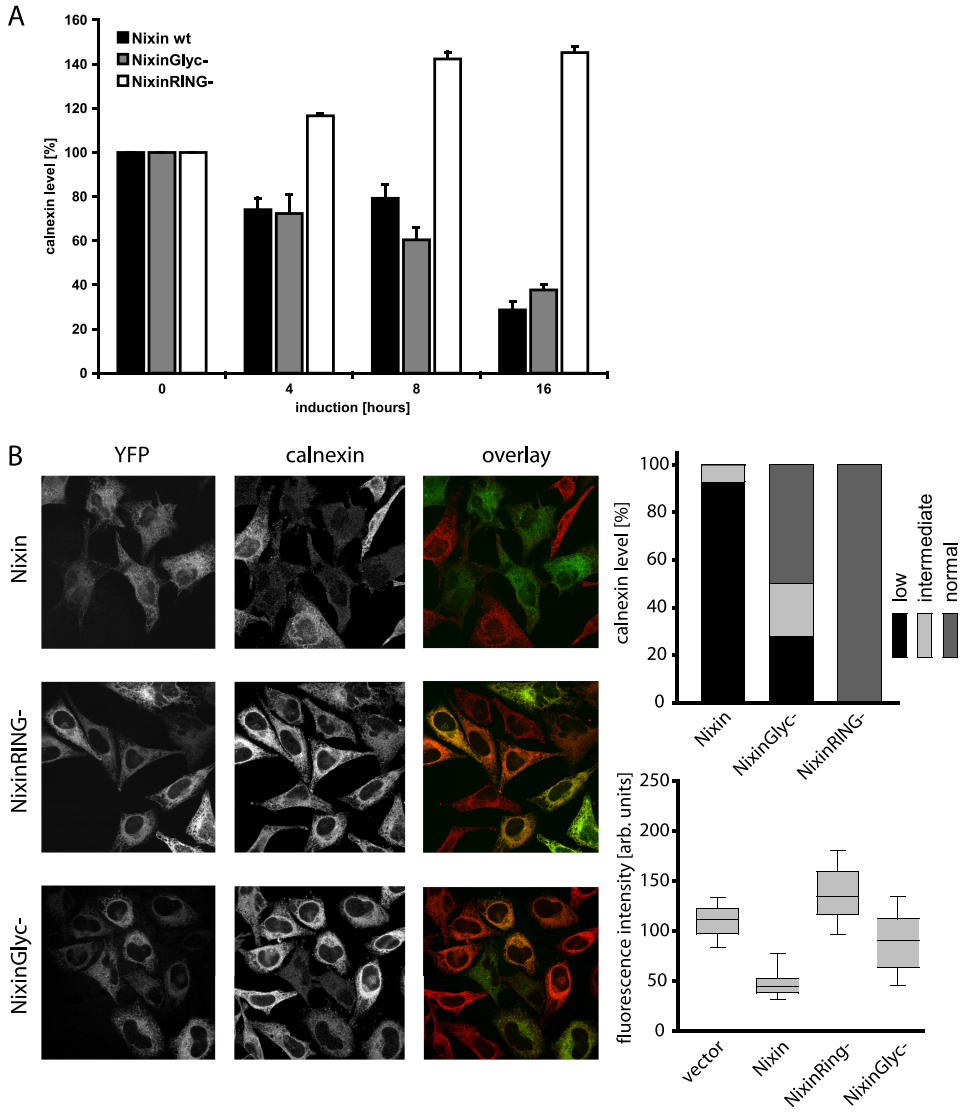

FIGURE 5. **Activity of Nixin toward calnexin is glycosylation-independent.** *A,* FlpIn TRex 293 cells permanently transfected with wild type Nixin, Nixin^{RING-}, and Nixin^{Glyc-} were induced with tetracycline for the indicated times or left untreated and then analyzed by Western blot using anti-calnexin and anti-actin antibodies. Protein levels were quantified using an infrared fluorescence-based laser scanner, and calnexin levels were normalized to actin loading control (n = 3). *B,* HeLa cells were transfected with expression constructs for Nixin, Nixin^{RING-}, and NixinΔ1/2/3GS (Nixin^{Glyc-}), fixed, and immunostained with anti-calnexin antibody. Confocal images were also scored for cells expressing "normal" levels of calnexin, and those depleted of this protein (*bar graph,* median of four experiments with 90 < n <130; calnexin levels in untransfected cells were considered normal). In addition, the fluorescence intensity of confocal images was measured using MetaMorph software and blotted as a *box graph* where the *box* represents the range of fluorescence of the 25 percentile with the central line marking the median fluorescence of all cells measured, although the range bars represent the 95 percentile of all cells measured (n >130).

expression, a ladder-like pattern of calnexin mobility on SDS-PAGE was clearly detectable, suggesting increased calnexin ubiquitination following Nixin expression. This pattern was most prominent between 5 and 7 h after Nixin induction (Fig. 6*C*). The modification of calnexin consistent with ubiquitination was followed by a decrease in calnexin levels, evident at 7 or 8 h after Nixin induction (Fig. 6*C*).

Ubiquitinated ERAD substrate proteins are recognized by the AAA-ATPase p97, which is thought to provide the force for the retrotranslocation of ubiquitinated proteins from the ER for proteasomal degradation in the cytoplasm (33). We tested whether the Nixin-dependent regulation of calnexin levels shares this part of the degradation machinery with the prototypical ERAD ubiquitin ligases SYVN1/hHrd1 and gp78. Nixin FlpIn T-Rex 293 cells were transfected with expression constructs for p97 or an ATPase-negative version of p97 (p97$^{ATPase-}$; Fig. 6*D*). At 3 h of Nixin induction with tetracycline, the mobility pattern of calnexin was analyzed by Western blotting. Although the transfection of wild type p97 did not markedly change the amount of the higher molecular weight calnexin ladder compared with control cells, transfection of an inactive version of p97 caused an at least 2-fold accumulation of higher molecular weight calnexin ladders (Fig. 6*D, bottom panel*), consistent with a block of retrotranslocation of ubiquitinated calnexin from the ER.

We then used coimmunoprecipitation to assess a possible interaction between Nixin and calnexin. Wild type Nixin, Nixin^{RING-}, or Nixin^{Glyc-} was immunopurified from cellular lysates obtained from 293 TRex FlpIn cells with a lysate from cells expressing the unrelated protein HaloTag used as control

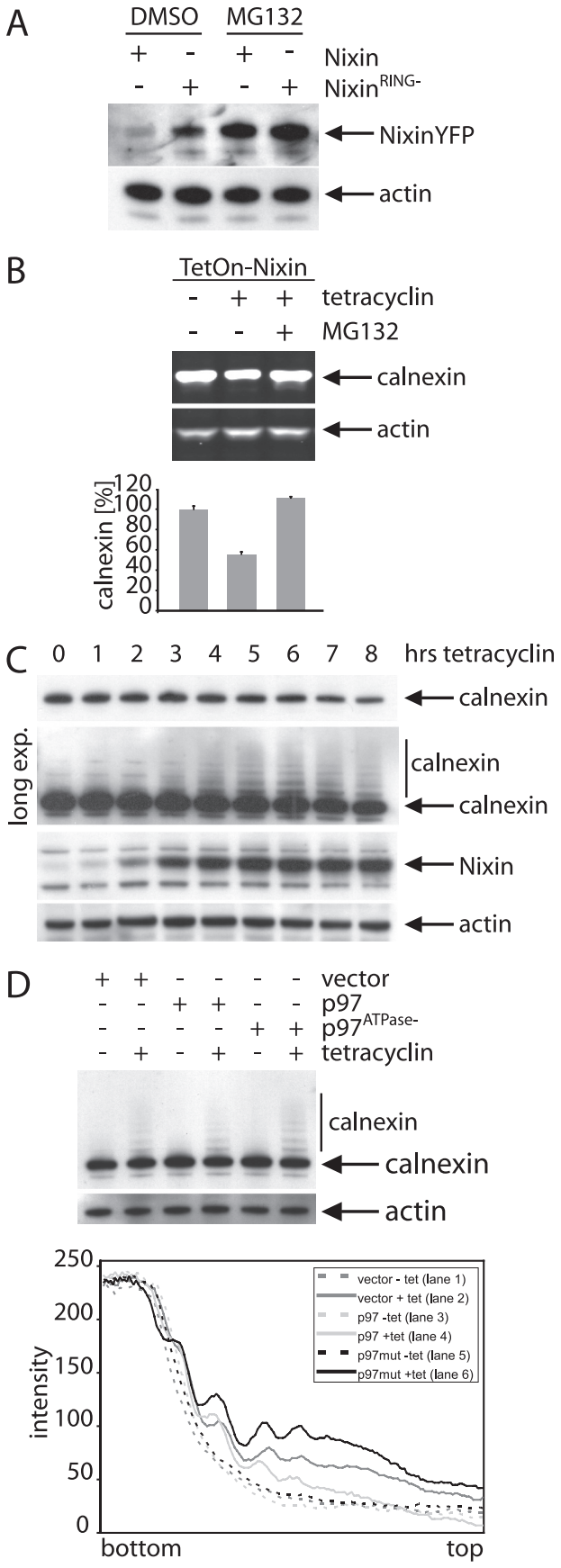

FIGURE 6. **Nixin regulates ubiquitin- and proteasome-dependent turnover of calnexin.** *A,* HeLa cells transfected with Nixin-YFP or Nixin^{RING-}-YFP expression constructs were treated for 5 h with the proteasome inhibitor MG132 or mock-treated with DMSO. Anti-GFP antibodies were used to analyze the levels of Nixin protein by Western blot. Actin served as loading control. *B,* Nixin induces the proteasome-dependent degradation of calnexin. FlpIn TRex 293 cells permanently transfected with wild type Nixin under the control of the Tet-On promoter were treated with tetracycline for 8 h and then treated with the proteasome inhibitor MG132 or mock-treated with vehicle for 6 h (MG132 was added 2 h after tetracycline). Uninduced cells served as control. The levels of calnexin were determined by infrared-based quantitative Western blot, normalized to actin levels and compared with control cells. *C,* Nixin induces calnexin ubiquitination in a time-dependent manner. FlpIn TRex 293 cells permanently transfected with wild type Nixin under the control of the Tet-On promoter were induced with tetracycline for the indicated time (0–8 h) and analyzed by Western blot. Two expositions for calnexin are displayed to show the degradation of calnexin (*1st panel*) as well as the modification of calnexin (*2nd panel*). *D,* Nixin induces p97-dependent calnexin degradation. The cell line described in *B* and *C* was transfected with expression constructs for p97, an ATPase-inactive mutant of p97 (p97$^{ATPase-}$), or with vector as control, followed by 3 h of induction of Nixin expression with tetracycline, and then analyzed by Western blot. Note the at least 2-fold increase of ubiquitinated calnexin in the *6th lane* compared with the *2nd* and *4th lanes*. Ubiquitinated species of calnexin were also revealed using densitometry (*bottom panel*).

(Fig. 7*A*). Analyzing precipitated proteins by Western blot using biotinylated anti-Nixin antibodies, we confirmed the purification of ectopically expressed Nixin, Nixin^{RING-}, and Nixin^{Glyc-}. In addition, a band the size of Nixin was detected in the control precipitation consistent with the purification of endogenous Nixin from this lysate. As shown in Fig. 7*A* (*3rd panel*) using anti-calnexin antibodies, calnexin specifically copurified with Nixin in all samples compared with controls. This result hints to a RING finger and glycosylation-independent interaction between Nixin and calnexin. However, we cannot exclude the possibility that calnexin only interacts with endogenous Nixin under these conditions. We therefore performed the reverse experiment and immunopurified calnexin using anti-calnexin antibodies from cellular lysates containing Nixin, Nixin^{RING-}, or Nixin^{Glyc-}. As shown in Fig. 7*B*, purification of calnexin specifically resulted in the copurification of wild type Nixin, Nixin^{RING-}, as well as Nixin^{Glyc-} compared with controls. These data confirm a physical interaction between Nixin and calnexin that is independent of the glycosylation status and activity of Nixin.

To test the role of ubiquitination in the regulation of calnexin levels, we asked whether calnexin is a target for ubiquitination. To this end, calnexin was immunopurified using anti-calnexin antibodies from native lysates obtained from MG132-treated cells expressing FLAG-ubiquitin alone or together with tetracycline-inducible Nixin (Fig. 7*C*). Calnexin copurifying FLAG-ubiquitin was analyzed using anti-FLAG antibodies. We found ubiquitinated protein consistent in size with calnexin-ubiquitin and/or ubiquitinated proteins noncovalently interacting with calnexin. Although this ubiquitination was detected in the absence of ectopically expressed Nixin, induction of Nixin expression increased the amount of FLAG-ubiquitin copurifying with calnexin around 1.3-fold. The analysis of immunopurified calnexin with anti-calnexin antibodies by Western blot (Fig. 7*C*, *upper right panel*) revealed high molecular bands that increased considerably in size upon induction with tetracycline consistent with Nixin-induced calnexin ubiquitination. In sum, the data presented in Figs. 6 and 7 are consistent with a model whereby the ubiquitin ligase Nixin recognizes and ubiquitinates calnexin, which in turn would lead to the dislocation of

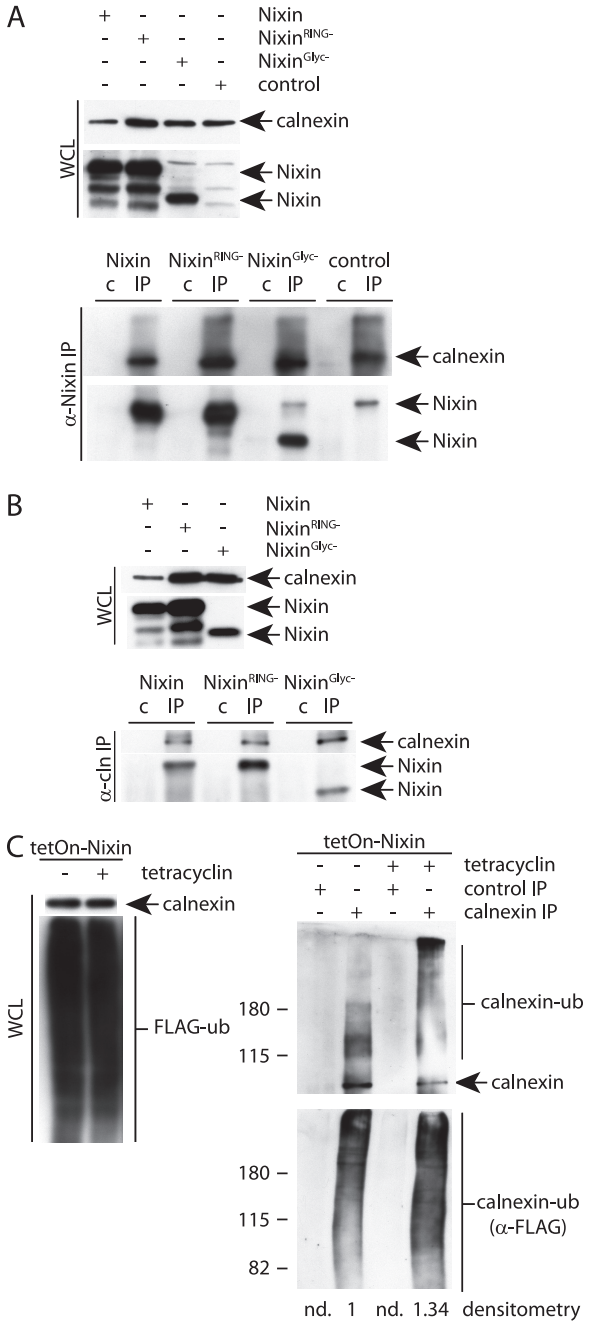

FIGURE 7. **Calnexin is a target for ubiquitination.** *A,* Nixin, Nixin^{RING-}, or Nixin^{Glyc-} were immunoprecipitated (*IP*) from FlpIn TRex 293 protein lysates, and precipitates were analyzed with anti-calnexin and biotinylated anti-Nixin antibodies. Cells expressing the unrelated protein HaloTag (Promega) as well as omission of anti-Nixin antibody during purification served as control (labeled *c*). Please note anti-Nixin reactive band(s) in the control lysate and the control purification are consistent in size with endogenous Nixin, which interacts with calnexin. *WCL*, whole cell lysate. *B,* calnexin was immunopurified from cell lysates obtained from FlpIn TRex 293 cells expressing Nixin, Nixin^{RING-}, or Nixin^{Glyc}. Immunoprecipitates were analyzed for the presence of Nixin using biotinylated anti-Nixin antibody. Incubation of lysates with protein A/G beads but without anti-calnexin antibodies (labeled *c*) served as control. *C,* Nixin enhances calnexin ubiquitination. Calnexin was immunoprecipitated from Nixin FlpIn TRex 293 cells transfected with a $^{FLAG3\times}$ubiquitin (*ub*) expression construct and then treated with tetracycline for 6 h to induce Nixin expression or left untreated. Omission of anti-calnexin antibodies in the purification served as control. Detection of FLAG-ubiquitin in calnexin precipitates was used to assess calnexin ubiquitination. Densitometric quantification was performed using ImageJ (National Institutes of Health). Please also note the increase in high molecular weight calnexin in the anti-calnexin Western blot (*upper panel*). *nd* means not determined.

calnexin from the ER by p97 AAA-ATPase and subsequent degradation by the proteasome.

DISCUSSION

Comparing Proteomics Approaches to the Findings of the RTM Screen—The protein content of cellular organelles is of great interest and has sparked numerous studies on organellar proteomes (34, 35). In these studies, after purification of the organelle of interest, proteins were identified using mass spectrometry. Although these large scale proteomic approaches are valuable in analyzing organelles, hydrophobic membrane-bound proteins still pose technical difficulties for identification by mass spectrometry (36). We compared the localization data described here with the organellar proteomics results, as well as with localization data from the NCBI gene data base (Table 1). Because most published reports show data from mouse- or rat-derived samples, we collected all available sequence information and used the NCBI BLAST program to find the homologous human proteins. We then queried the NCBI gene data base and mapped the published accession numbers from various sources to the corresponding NCBI gene ID. In addition, to incorporate more localization data into the comparisons of the RTM list with previously published data, we performed a search of the NCBI gene data base restricted to localization to the ER. This resulted in the identification of 594 ER-associated gene products. Of these proteins, only four were RTMs, although we identified 24 RTMs at the ER. The most comprehensive published evaluation of mouse membrane-bound organelles (34) revealed the localization of 1398 proteins. This study covered most membrane systems inside a eukaryotic cell and identified one RTM (gp78/AMFR) in the ER.

One can speculate that tissue- and cell type-specific expression of different RTMs, their potential low abundance due to self-degradation, as well as technical difficulties posed by hydrophobic proteins might explain the absence of most ER localized RTMs in these proteomic studies. The 24 ER-localized RTMs described here expand the family of known ER-resident RING domain proteins by 4-fold. We believe that these findings are likely to accelerate future studies of protein quality control in the ER.

Interestingly, when analyzing the 54 RTMs, besides the RING domain only so-called PA domains could be identified as potential protein/protein interaction motifs. Of those eight RTMs with a PA domain (supplemental Fig. S3), four were found by us to localize to the ER, and all share the same structural organization with the PA domain near the N terminus separated from the C-terminal RING domain by one predicted transmembrane region. Except for RNF130, the same topology is shared by the other RTMs on other organelles. It seems to be a unifying theme of this sub-class of RTMs to couple substrate recognition via the PA domain with RING-dependent ubiquitination across membranes.

A Model for the Function of Nixin—Calnexin plays a central part in the processing of newly synthesized proteins destined for folding and glycosylation in the ER. It recognizes partially folded proteins based on their glycosylation status and allows such proteins to spend additional time in the folding friendly environment of the ER by preventing their removal by ERAD

TABLE 1

Comparison of the RTM screen to published localizations

The NCBI gene database was searched for human genes localized to the ER, and this list was compared with the inventory of all ER-localized RTMs. In addition, the RTM list was matched up to a published proteome of the ER (34). ND means not determined.

Organelle	Reference	No. of proteins	TMHMM prediction	RING finger	Intersection with RTM list
ER	NCBI gene	594	ND	ND	RNF139, AMFR, RNF47,RNF112
ER	34	228	82	1	AMFR/gp78
ER/Golgi	34	219	41	0	

(10). Therefore, the time calnexin client proteins are allowed to reside in the ER is determined by the relative amount of folding proteins, the level of calnexin, and the glycosidase/deglycosidase activity in the ER. In order for the cell to efficiently fold proteins and keep the flux of proteins through the ER in homeostasis, the time folding proteins are allowed to spend in the ER must be under tight control. This can be achieved by the initiation of UPR in case of protein overload in the ER. In addition, as we propose here, Nixin-dependent dynamic regulation of calnexin levels might also contribute to the modulation of protein traffic through the ER.

The data presented in this study suggest a model where Nixin acts as a gauge for the rate of protein flux through the ER by keeping calnexin at the right concentration. We show that Nixin acts as ubiquitin ligase for calnexin (see Figs. 6 and 7). Whether Nixin is also a calnexin client protein is unknown, however, based on the activity of Nixin^{Glyc-} toward calnexin and the glycosylation-independent interaction between these two proteins, the recognition of calnexin through Nixin does not rely on glycosylation. In addition to the RING finger domain, Nixin also contains a PA domain that is implicated in protein/protein interaction (37), and based on the topology of Nixin, recognition of calnexin by Nixin via the PA domain in the ER lumen and subsequent ubiquitination on the short cytoplasmic lysine-rich tail of calnexin seem plausible.

Another feature of Nixin compatible with a regulatory role in maintaining the folding capacity of the cells is its own instability. As shown in Fig. 6*A*, compared with Nixin^{RING-}, wild type Nixin is quite unstable. This instability is a common feature of ubiquitin ligases and might help to regulate Nixin levels according to the availability of free calnexin.

Nixin-induced degradation of calnexin suggests a physiological role for Nixin during a time when the cell contains calnexin in excess. In addition to the above-mentioned steady state regulation, this might be the case after a cell has suffered ER stress and initiated the unfolded protein response. UPR is known to shut down protein synthesis but also to promote expression of the ER protein folding machinery, including calnexin. After having overcome ER stress and restoration of normal conditions, the UPR has to be attenuated by bringing down the chaperone concentration to pre-stress levels. One might speculate that under these conditions Nixin might mediate removal of abundant calnexin. Because calnexin is known to retain proteins in the ER destined for other cellular compartments, it is conceivable that calnexin levels must be tightly controlled, and elevated levels beneficial during ER stress might be harmful under normal conditions. One example of detrimentally high levels of calnexin are MCF7 breast cancer cells, where the upregulation of calnexin is used to evade ER stress-induced apoptosis (38). Therefore, attenuation of UPR by Nixin might serve to restore normal, pre-stress protein traffic through the ER.

Concluding Remarks—Taken together, sampling all human membrane-anchored RING finger ubiquitin ligases led to the discovery of a novel regulatory mechanism for calnexin. Future analysis of other RTMs localized to the ER on the levels of other chaperones like BiP, for example, might reveal additional regulatory networks that keep the UPR under tight control. Beyond UPR, ER-localized RTMs are prime candidates to be regulators of other ER functions, and RTMs localized to other cellular membrane systems underline the importance of ubiquitin-dependent protein degradation for maintaining cellular organelle function.

Acknowledgments—We thank James W. Nagle and Debbie Kaufmann from NINDS DNA sequencing facility, Carolyn Smith from NINDS, Beat Erne from Department of Biomedicine light imaging facilities, and Susan V. Smith for technical support. We also thank S. Fang for kindly providing the p97 plasmids and C. Garrison Fathman for making the FLAG-ubiquitin plasmid available.

REFERENCES

1. Kostova, Z., Tsai, Y. C., and Weissman, A. M. (2007) *Semin. Cell Dev. Biol.* **18,** 770–779
2. Harding, H. P., Calfon, M., Urano, F., Novoa, I., and Ron, D. (2002) *Annu. Rev. Cell Dev. Biol.* **18,** 575–599
3. Ron, D., and Walter, P. (2007) *Nat. Rev. Mol. Cell Biol.* **8,** 519–529
4. Hirsch, C., Jarosch, E., Sommer, T., and Wolf, D. H. (2004) *Biochim. Biophys. Acta* **1695,** 215–223
5. Meusser, B., Hirsch, C., Jarosch, E., and Sommer, T. (2005) *Nat. Cell Biol.* **7,** 766–772
6. Bordallo, J., Plemper, R. K., Finger, A., and Wolf, D. H. (1998) *Mol. Biol. Cell* **9,** 209–222
7. Carvalho, P., Goder, V., and Rapoport, T. A. (2006) *Cell* **126,** 361–373
8. Denic, V., Quan, E. M., and Weissman, J. S. (2006) *Cell* **126,** 349–359
9. Ye, Y. (2006) *J. Struct. Biol.* **156,** 29–40
10. Hebert, D. N., Garman, S. C., and Molinari, M. (2005) *Trends Cell Biol.* **15,** 364–370
11. Ruddock, L. W., and Molinari, M. (2006) *J. Cell Sci.* **119,** 4373–4380
12. Kikkert, M., Doolman, R., Dai, M., Avner, R., Hassink, G., van Voorden, S., Thanedar, S., Roitelman, J., Chau, V., and Wiertz, E. (2004) *J. Biol. Chem.* **279,** 3525–3534
13. Fang, S., Ferrone, M., Yang, C., Jensen, J. P., Tiwari, S., and Weissman, A. M. (2001) *Proc. Natl. Acad. Sci. U.S.A.* **98,** 14422–14427
14. Kreft, S. G., Wang, L., and Hochstrasser, M. (2006) *J. Biol. Chem.* **281,** 4646–4653
15. Younger, J. M., Chen, L., Ren, H. Y., Rosser, M. F., Turnbull, E. L., Fan, C. Y., Patterson, C., and Cyr, D. M. (2006) *Cell* **126,** 571–582
16. Lerner, M., Corcoran, M., Cepeda, D., Nielsen, M. L., Zubarev, R., Pontén, F., Uhlén, M., Hober, S., Grandér, D., and Sangfelt, O. (2007) *Mol. Biol. Cell* **18,** 1670–1682
17. Zhang, Q., Meng, Y., Zhang, L., Chen, J., and Zhu, D. (2009) *Cell Res.* **19,** 348–357

18. Pind, S., Riordan, J. R., and Williams, D. B. (1994) *J. Biol. Chem.* **269,** 12784–12788
19. Oliver, J. D., Hresko, R. C., Mueckler, M., and High, S. (1996) *J. Biol. Chem.* **271,** 13691–13696
20. Lorenz, H., Hailey, D. W., Wunder, C., and Lippincott-Schwartz, J. (2006) *Nat. Protoc.* **1,** 276–279
21. Huibregtse, J. M., Scheffner, M., Beaudenon, S., and Howley, P. M. (1995) *Proc. Natl. Acad. Sci. U.S.A.* **92,** 2563–2567
22. Joazeiro, C. A., Wing, S. S., Huang, H., Leverson, J. D., Hunter, T., and Liu, Y. C. (1999) *Science* **286,** 309–312
23. Joazeiro, C. A., and Weissman, A. M. (2000) *Cell* **102,** 549–552
24. Okumoto, K., Itoh, R., Shimozawa, N., Suzuki, Y., Tamura, S., Kondo, N., and Fujiki, Y. (1998) *Hum. Mol. Genet.* **7,** 1399–1405
25. Altschul, S. F., Gish, W., Miller, W., Myers, E. W., and Lipman, D. J. (1990) *J. Mol. Biol.* **215,** 403–410
26. Sonnhammer, E. L., von Heijne, G., and Krogh, A. (1998) *Proc. Int. Conf. Intell. Syst. Mol. Biol.* **6,** 175–182
27. Kersey, P. J., Duarte, J., Williams, A., Karavidopoulou, Y., Birney, E., and Apweiler, R. (2004) *Proteomics* **4,** 1985–1988
28. Wheeler, D. L., Barrett, T., Benson, D. A., Bryant, S. H., Canese, K., Chetvernin, V., Church, D. M., DiCuccio, M., Edgar, R., Federhen, S., Geer, L. Y., Helmberg, W., Kapustin, Y., Kenton, D. L., Khovayko, O., Lipman, D. J., Madden, T. L., Maglott, D. R., Ostell, J., Pruitt, K. D., Schuler, G. D., Schriml, L. M., Sequeira, E., Sherry, S. T., Sirotkin, K., Souvorov, A., Starchenko, G., Suzek, T. O., Tatusov, R., Tatusova, T. A., Wagner, L., and Yaschenko, E. (2006) *Nucleic Acids Res.* **34,** D173–D180
29. Fujii, T., Tamura, K., Copeland, N. G., Gilbert, D. J., Jenkins, N. A., Yomogida, K., Tanaka, H., Nishimune, Y., Nojima, H., and Abiko, Y. (1999) *Genomics* **57,** 94–101
30. Ain, Q., Nazli, S., Riazuddin, S., Jaleel, A. U., Riazuddin, S. A., Zafar, A. U., Khan, S. N., Husnain, T., Griffith, A. J., Ahmed, Z. M., Friedman, T. B., and Riazuddin, S. (2007) *Hum. Genet.* **122,** 445–450
31. Kobata, A. (1979) *Anal. Biochem.* **100,** 1–14
32. Laney, J. D., and Hochstrasser, M. (2002) in *Current Protocols in Protein Science* (Coligan, J. E., Dunn, B. M., Speicher, D. W., and Wingfield, P. T., eds) pp. 1–11, Wiley, New York
33. Raasi, S., and Wolf, D. H. (2007) *Semin. Cell Dev. Biol.* **18,** 780–791
34. Foster, L. J., de Hoog, C. L., Zhang, Y., Zhang, Y., Xie, X., Mootha, V. K., and Mann, M. (2006) *Cell* **125,** 187–199
35. Yates, J. R., 3rd, Gilchrist, A., Howell, K. E., and Bergeron, J. J. (2005) *Nat. Rev. Mol. Cell Biol.* **6,** 702–714
36. Santoni, V., Molloy, M., and Rabilloud, T. (2000) *Electrophoresis* **21,** 1054–1070
37. Mahon, P., and Bateman, A. (2000) *Protein Sci.* **9,** 1930–1934
38. Delom, F., Emadali, A., Cocolakis, E., Lebrun, J. J., Nantel, A., and Chevet, E. (2007) *Cell Death Differ.* **14,** 586–596